Low-Pressure Carbon Dioxide Enhanced Polymer Chain Mobility below the Bulk Glass Transition Temperature

Yong Yang,[†] Mark Ming-Cheng Cheng,[‡,||] Xin Hu,[§] Dehua Liu,[†] Richard J. Goyette,[⊥,#] L. James Lee,*[,†] and Mauro Ferrari[‡,||]

Department of Chemical and Biomolecular Engineering, Division of Hematology and Oncology, Department of Internal Medicine, and Department of Mechanical Engineering, The Ohio State University, Columbus, Ohio 43210, and Argonne National Laboratory, Argonne, Illinois 60439

Received July 3, 2006; Revised Manuscript Received December 14, 2006

ABSTRACT: The effects of low-pressure carbon dioxide (CO_2) on chain mobility of polystyrene (PS) and poly(methyl methacrylate) (PMMA) thin films coated on a solid surface were studied using PS/deuterated PS/Si and PMMA/deuterated PMMA/SiO_2 configurations. The time evolution of chain diffusion below the bulk glass transition temperature (T_g) with and without CO_2 was measured by neutron reflectivity. It was found that polymer chains at the interface can self-diffuse at a temperature below their bulk T_g because of higher surface chain mobility and that adding CO_2, even at low pressures, can greatly enhance the chain mobility. When the interactions between the polymer chains and the substrate are weak as in the PS/Si configuration, the confining effects of the substrate are not significant, while in the case of the PMMA/SiO_2 configuration the interactions are strong enough to confine polymer chains onto the substrate at the nanoscale. Introducing CO_2 tends to alleviate this confining effect.

Introduction

The dynamics of polymer thin films have attracted increased attention due to scientific interest as well as their importance in coatings, electronic packaging, dielectric layers, composites, and biocompatible materials.[1] Emerging polymer-based nanotechnology requires a comprehensive understanding of molecular dynamics of confined polymers at the nanoscale. As structures are made smaller and smaller, it becomes critical to understand how thermal and mechanical properties of materials vary near the proximity of the interface and how to manipulate these properties.[2]

It has been reported that polymer properties at the free surface and near the polymer−substrate interface may differ from those in the bulk.[3] For example, the glass transition temperature (T_g) is largely depressed at the surface when the substrate effect is weak or negligible,[4,5] and Kajiyama et al.[6] observed a high chain mobility near the polystyrene (PS) surface below the bulk T_g.

In the presence of favorable enthalpic interactions between the polymer and the substrate, the chain conformations near the substrate can be highly confined, thus retarding the chain mobility and elevating the T_g.[7] In poly(methyl methacrylate) (PMMA)/deuterated PMMA (*d*PMMA) bilayers near the silicon oxide surface, Lin et al.[8] observed that the effective diffusion coefficient dramatically decreased when the *d*PMMA layer was less than $3R_g$ (the radius of gyration of the bulk polymer) and approached the bulk interdiffusion rate when the layer thickness was greater than $5R_g$. Depending on the strength of polymer−substrate interactions, the confining effect could reach a longer range.[9] Molecular dynamics simulation also verified this long-range confining effect.[10]

In addition to using elevated temperatures or external energy stimulation, supercritical carbon dioxide (CO_2) has been introduced to enhance the chain mobility and even desorb the polymer from the substrate surface. CO_2 molecules are small and linear and can rapidly diffuse into polymers and cause plasticizing. The plasticizing effect, which controls the mobility of the polymer chains, can be tuned by adjusting the CO_2 pressure.[11] Moreover, CO_2 may interact with the polymer and the substrate and hence shield the polymer−substrate interactions.[12] Gupta et al.[13] have observed nearly an order of magnitude increase in the diffusivity of PS upon increasing the sorbed volume fraction of CO_2 from 8.9 to 11.3 wt % at 62 °C.

Our previous studies have shown that CO_2, even at low pressures, can enhance the interfacial bonding of polymers far below the bulk T_g without deforming structures at the micro/nanoscale.[14−16] In this study, we investigate the enhancement of chain mobility by low-pressure CO_2 below the bulk T_g, the confining effects of substrates on polymers, and the effects of CO_2 and substrate confinement on polymer chain mobility. The ultimate goal is to facilitate polymer nanofabrication at low temperatures using low-pressure CO_2 as a processing aid.

Experimental Section

The materials used include hydrogenated PS (*h*PS; $M_n = 214\,000$, $M_w/M_n = 1.03$), deuterated PS (*d*PS; $M_n = 178\,000$, $M_w/M_n = 1.10$, $R_g = 113$ Å[17]), hydrogenated PMMA (*h*PMMA; $M_n = 212\,900$, $M_w/M_n = 1.06$), and deuterated PMMA (*d*PMMA; $M_n = 210\,500$, $M_w/M_n = 1.04$, $R_g = 145$ Å[18]). All of the materials were supplied by Polymer Source Inc. The 50 mm diameter Si wafers (Montco-Silicon Technologies, Inc.) were first cleaned by immersion in piranha solution for 15 min at 120 °C and then dipped for 10 s in a buffer oxide etchant. A dry silicon oxide layer was thermally grown on some wafers at 1050 °C for 2.7 h to a thickness of 1150 Å, designated as the SiO_2 wafers.

The solutions of the polymer in toluene (0.5−1.5 wt %) were filtered through a 0.1 μm inorganic membrane filter (Whatman, Anotop 25) and spin-coated onto the substrate to form thin films. In the *h*PS/*d*PS/Si configuration, the thickness of the *d*PS layer ranges from 113 to 738 Å ($1.0-6.5R_g$). For the *h*PMMA/*d*PMMA/

* Corresponding author. E-mail: lee.31@osu.edu.
[†] Department of Chemical and Biomolecular Engineering, OSU.
[‡] Division of Hematology and Oncology, Department of Internal Medicine, OSU.
[§] Department of Mechanical Engineering, OSU.
[⊥] Argonne National Laboratory.
[||] Present address: Nanomedicine, Institute of Molecular Medicine, 1825 Pressler St, Suite 537, The University of Texas Health Science Center at Houston, Houston, TX 77030.
[#] Present address: The Spallation Neutron Source, Oak Ridge National Laboratory, P.O. Box 2008, Oak Ridge, TN 37831.

10.1021/ma061492o CCC: $37.00
Published on Web 01/26/2007

SiO_2 configuration, the *d*PMMA layer thickness ranges from 124 to 603 Å ($0.86-4.2R_g$). Independently, an ~800 Å thick hydrogenated polymer film was spin-coated onto a SiO_2 wafer. The thickness of the films was determined by spectroscopic reflectometry (Nanospec 1000, Nanometrics Inc.), and the thickness variation was less than 10 Å over the dimension of the sample. The roughness of the films was characterized using atomic force microscopy (AFM) and confirmed to be less than 10 Å. After exposure to ambient conditions overnight, the polymer films were annealed at 150 °C for 12 h in a vacuum to remove the residual solvent and relax the residual stresses imposed by spin-coating. Annealing-induced dewetting was observed on the thinner polymer films, in particular the films having a thickness of about R_g. The portion of the dewetting area is very small compared with the entire surface and can be ignored,[19] which was further confirmed by comparing the neutron reflectivity of samples with and without dewetting (results not shown). The perimeter of the hydrogenated polymer film was scored with a blade, and then the film was floated off onto the surface of a 7:1 buffer oxide etchant (BOE). Subsequently, the film was rinsed with 18 MΩ·cm water and picked up onto the deuterated polymer film. Again, the residual water was removed by annealing the bilayer samples at 65 °C in vacuum for 5 h. The effect of the BOE on the thin film surface was carefully examined by using the AFM/nanoparticles method.[20,21] Monodispersed gold nanoparticles were placed on the polymer surfaces with and without the BOE treatment, followed by annealing at 70 °C in a vacuum for 5 h. No obvious difference in the apparent height of the nanoparticles was detected between these two surfaces, indicating that the BOE effect on the surface is negligible.

The bilayer samples were annealed at 70 °C in a vacuum or under various CO_2 (99.99% purity, Praxair, Inc.) pressures for a series of prespecified times. Upon completion of the annealing, ice water was used to quench the samples, followed by a slow-pressure release. After annealing, the sample was taken out and stored in a desiccator under ambient conditions prior to the neutron reflectivity measurements.

In order to compare the PS and PMMA systems, the annealing temperatures were fixed at 70 °C through this study. Their bulk T_gs were determined to be 100.2 °C for PS and 104.6 °C for PMMA using differential scanning calorimetry (TA DSC 2920). Plasticized with CO_2, PS has a bulk T_g of 90.6 °C under 1.38 MPa CO_2 pressure, determined by using TA DSC 2920 equipped with a high-pressure cell. The bulk T_g of PMMA is measured to be 91.0 °C under 1.72 MPa CO_2, and this pressure was used to assist annealing the samples. This choice of the CO_2 pressure ensures very close bulk T_gs for CO_2 plasticized polymers.

Specular neutron reflectivity measurements were carried out using the unpolarized neutron reflectometer (POSY II) at the Intense Pulsed Neutron Source, Argonne National Laboratory, Argonne, IL. The incident neutrons with a broad wavelength distribution (1−16 Å) impinged on the sample at a glancing angle of 0.6° (or 0.45°) and 1.6° and a resolution of 3.0%. This angle range allowed for sufficient overlap of the data sets. Reflectivity data were fitted using the Parratt formalism assuming a multilayer model. On the basis of the slope at the midpoint of the fitted scattering length density vs thickness, the interfacial width can be calculated.[22]

Results and Discussion

Figure 1 shows the representative neutron reflectivity data with experimental error for *h*PS/*d*PS/Si configuration (having a *d*PS layer of 738 Å thick) at different annealing times. It is obvious that there is a nonzero interfacial width σ_0 at the annealing time $t = 0$. The interfacial width σ_t at a time t was corrected quadratically for the initial interfacial width σ_0.[23] The time evolution of the interfacial width σ_t is plotted in Figure 2. It was found that PS chains could diffuse across the interface at 70 °C in vacuum and the interfacial width gradually increased. It is well-known that the T_gs of PS thin films are largely depressed and decrease with reduced thickness. Keddie et al.

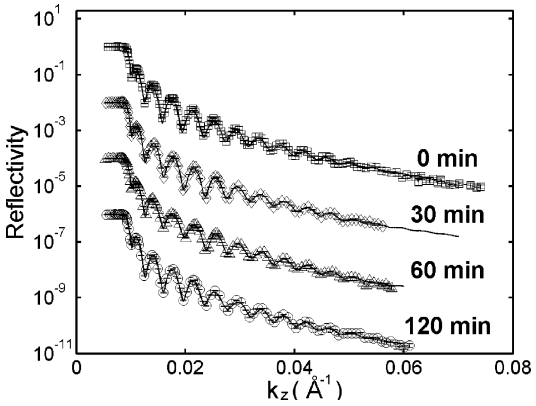

Figure 1. Neutron reflectivity data vs momentum transfer k_z of *h*PS/*d*PS/Si samples after annealing at different times. Here the thickness of *h*PS is ~800 Å, and that of *d*PS is 738 Å. The reflectivity curves have been offset vertically for clarity. The solid lines represent the respective calculated reflectivity profiles.

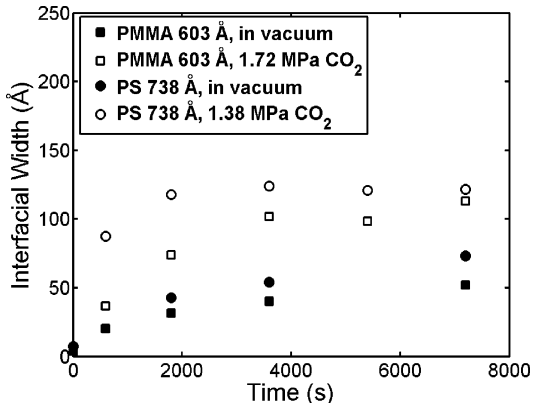

Figure 2. Time evolution of the interfacial width of the bilayers with the thickest bottom layers at 70 °C, with and without CO_2. The initial interfacial widths are also plotted as reference.

measured the T_g of PS on bare Si wafers and fitted the data to an empirical equation, $T_g(h) = T_g(\text{bulk})[1 - (A/h)^\delta]$, where $T_g(h)$ is the thickness (h)-dependent T_g of the polymer film; A (32 ± 6 Å for PS) and δ (1.8 ± 0.2 for PS) are the characteristic length and the exponent, respectively.[4] For the PS used (T_g(bulk) = 100.2 °C), the T_g for this PS film (738 Å) is 99.8 °C, indicating that the PS chains have a significant mobility at the interface.

The AFM/nanoparticle method was applied to probe the mobile surface layer of the polymer.[20,21] The measurements are described in detail elsewhere[16] and summarized here. Briefly, a polymer film is spin-coated onto a silicon wafer with a surface roughness in the range 1−2 nm. Monodispersed gold nanoparticles (20.3 ± 1.1 nm, Ted Pella, Inc.) are then placed onto the polymer surface to serve as the probe. After annealing at a prespecified temperature in a vacuum or under CO_2 pressure for 5 h, the system reaches an equilibrium state, and the apparent height of the nanoparticles embedded onto the surface is measured using AFM. The mobile surface layer at the annealing temperature can be determined from the difference between the particle size and the apparent height. Although this method is contentious when trying to define a true T_g and the measured temperature is not the exact local T_g,[24,25] it is much closer to the real value of the local T_g than that obtained from thin film studies; moreover, this method also shows the depth-dependent T_g trend. The AFM measurements of the gold nanoparticles reveal that there is a mobile surface layer of 25 ± 11 Å at 70 °C.[16] Upon formation of the bilayer sample, there is no chain

entanglement or less chain entanglement than the bulk between the surfaces of *d*PS and *h*PS films. The high mobility at the interface allows the polymer chain to diffuse into the opposite side and form segmental chain entanglement. It is postulated that the chain entanglement density (and thus the T_g) in the mixed interface increases with diffusion. Finally, the T_g reaches the annealing temperature (70 °C), and the diffusion process stops.

In the presence of 1.38 MPa CO_2, AFM measurements of the gold nanoparticles indicate that the thickness of the mobile surface layer increased from 25 ± 11 Å in a vacuum to 103 ± 12 Å at 1.38 MPa CO_2. Figure 2 shows that the PS chain diffusion was greatly enhanced and reached equilibrium in about 60 min in the presence of 1.38 MPa CO_2. The equilibrium interfacial width of about 122 Å is close to the R_g of PS molecules, indicating that the polymer chain movement is still limited to segmental diffusion only. Translational diffusion does not occur in this case. The presence of CO_2 at 70 °C has enhanced the chain mobility at the interface, but not enough to reach the "flow" state.

For the PS used in this study, the bulk reptation time is scaled to be 509.4 min at 120 °C according to its molecular weight dependence.[19] The reptation time at 70 °C should be much longer than 509.4 min, indicating that the PS chains moved in the segmental mode over the time in vacuum in this study (the longest diffusion time is 120 min). Introducing CO_2 facilitated this segmental movement and shortened the time required to reach equilibrium to about 60 min.

A similar trend was observed for the *h*PMMA/*d*PMMA/SiO_2 configuration as shown in Figure 2. It is linearly interpolated from Pham' studies that the T_g of the PMMA film (603 Å) is about 129 °C in vacuum, and a CO_2 pressure of 1.72 MPa depresses the T_g by about 25 °C.[12] The T_gs are still higher than the annealing temperature, confirming the existence of a mobile surface layer. Recall that both the PS and the PMMA samples have the thickest bottom layer. At such a long distance, the effects of the substrate are not strong, and the low-pressure CO_2 can significantly enhance chain mobility near the polymer surfaces.

CO_2 absorbed into the polymer thin films could swell the films. We measured absorption of CO_2 in PMMA films supported on SiO_2 at 70 °C and 1.72 MPa CO_2 pressure using a Rubotherm magnetic suspension balance. The thickness of PMMA films varied from 15 to 92 nm. It was found that all of the systems reached equilibrium after 10−20 min (results not shown), which is consistent with the observation from Pham et al.[12] At the low CO_2 pressures studied, the maximum equilibrium swelling was estimated to be less than 3% for the PMMA[26] and negligible for the PS films.[27] Thus, the dimensional change resulting from CO_2 absorption for our PS films is insignificant, but there could be 20−25% error for our PMMA films.

When the thickness of the bottom layers was reduced below R_g, the confining effect of the substrate became clear. In the case of the thinnest *d*PS layer (113 Å or 1.0R_g), Figure 3 shows that PS chains gradually diffused across the interface as time increased. This diffusion is slower than that for the thickest bottom layer configuration (Figure 2). Under 1.38 MPa CO_2 pressure, the diffusion of PS chains was expedited as well. However, there was no obvious chain diffusion for the thinnest PMMA layer (124 Å or 0.86R_g). With a film thickness less than 2R_g (the dimension of the unperturbed chains), the polymer chains deviated from their unperturbed Gaussian conformation and oriented parallel to the substrate interface.[28] The polymer dynamics near the substrate surface are dominated by the

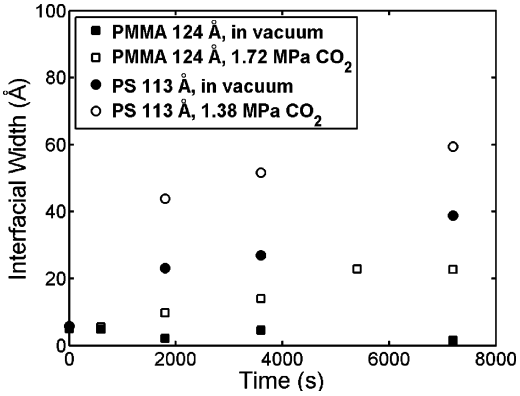

Figure 3. Time dependence of the interfacial width of the bilayers with the thinnest bottom layers at 70 °C, with and without CO_2. The initial interfacial widths are also plotted as reference.

repeating units in direct contact with the surface.[29] The Boltzmann factor for the removal of the chain is on the order of $\tau \approx \exp(-N_c E_a/kT)$, where N_c is the number of the repeating units contacting with the surface, E_a is the substrate−polymer segment interaction energy, k is Boltzmann's constant, and T is the absolute temperature.[23] Considering that both PS and PMMA have similar degrees of polymerization (1712 and 2105), their number of contact sites on the substrate are close to each other. It is reasonable to assume that their chain conformation on the substrate is similar at approximately the same film thickness. PS can diffuse away from the substrate while PMMA cannot, which indicates that the interaction energy or the enthalpic effects, instead of the entropic effects, are the primary factors of this confinement. On the silicon oxide surface, silanol groups form hydrogen bonds with the carbonyl oxygen of the PMMA chains.[30] The strong hydrogen bonding adsorbs the PMMA chains on the SiO_2 surface, restricting the chain mobility at the interface (Figure 3).

A large energy is needed to free an entire chain from the substrate into the bulk domain. It has been reported that even at a temperature as high as 150 °C, the interfacial width remained nearly constant with time for a very thin *d*PMMA layer (48 Å).[8]

Surprisingly, when 1.72 MPa CO_2 was introduced, there was an increase in the interfacial width for the thinnest PMMA layer (124 Å or 0.86R_g) (Figure 3). Pham et al.[12] attributed CO_2's capability in devitrificating PMMA thin films on the silicon oxide surface to three factors: CO_2-induced plasticization of polymer, CO_2 screening of the interactions between the PMMA carbonyl oxygen and the silanol group at the silicon oxide surface, and the collective effect from the surface adsorbed with CO_2. Considering the Boltzmann factor discussed previously, it is possible that CO_2 may interact with SiO_2 and decrease the substrate−polymer segment interaction energy E_a and/or the number of PMMA chain in contact with the substrate (i.e., lower N_c), thus activating the motion of the chains. By controlling the amount of CO_2 through pressure, the degree of enhanced chain mobility can be controlled to manipulate the motion of chains near the substrate surface.

In addition to the *h*PMMA/*d*PMMA/SiO_2 configurations with the thickest and the thinnest bottom layers, several samples with intermediate thickness were used to study the long-range effect of the substrate on chain mobility near the polymer surface. It is noted from Figures 2 and 3 that the interdiffusion of PMMA chains had not reached the equilibrium state without CO_2 after 120 min. In the presence of 1.72 MPa CO_2, both figures show

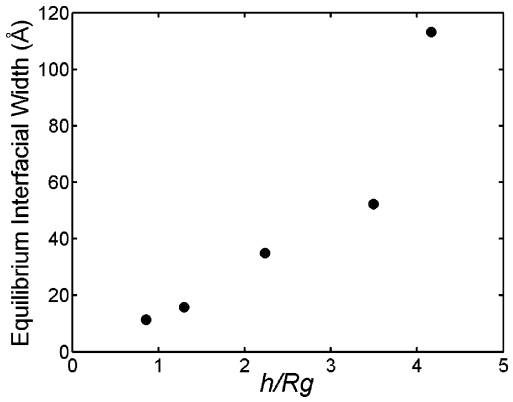

Figure 4. Long-range confining effects of the substrate on the polymer chain mobility. The film thickness h was normalized by the R_g of *d*PMMA.

a plateau, which implies the equilibrium state after 120 min annealing.

Figure 4 illustrates the dependence of the equilibrium interfacial width on the bottom *d*PMMA layer thickness under a CO_2 pressure of 1.78 MPa. Below $\sim 2R_g$, little interfacial width broadening was observed and the mobile surface layer was very thin. Beyond the thickness of $2R_g$, the equilibrium interfacial width increased from 31.4 Å at $2.2R_g$ to 113.2 Å at $4.2R_g$. Entanglements between polymer chains not in direct contact with the substrate and the less mobile loops and tails of the adsorbed polymer extend the substrate effect over a long distance.[8,31] On the other hand, the confining effect was gradually depressed with distance from the substrate, and CO_2's solvation effect resulted in broadening of the equilibrium interfacial width, indicating CO_2-induced broadening of the mobile surface layer.

Conclusions

In conclusion, a neutron reflectivity study was conducted on the dynamics of nanoconfined polymers with and without CO_2 below the bulk T_g. It was observed that polymer chains can diffuse discernibly in the surface region even below the bulk T_g. The presence of CO_2, even at low pressures, both expedited the diffusion process and increased the mobile surface layer. With a strong interaction between polymer chains and the substrate, the polymer chains can be confined onto the substrate. The confining effect may be reduced by introducing a low CO_2 pressure.

Dimensionally dependent polymer properties are critical for fabrication and application of polymer-based micro/nanoscale devices. In many biomedical applications, they are vital for the production and assembly of devices (e.g., biosensors, tissue engineering scaffolds) occurring in the presence of biomolecules and cells. Our other studies showed that polymeric micro/nanodevices can be assembled at low temperature and low CO_2 pressure,[14−16] even in buffer solutions with living cells.[32] This may lead to biologically benign micro/nanofabrication processes. In addition, when a solid substrate that has favorable interactions with the polymer is introduced into the matrix, the chain mobility of the polymer can be retarded or even totally confined onto the substrate, leading to enhanced physical and chemical properties. This phenomenon can be used to design high-performance nanocomposites, and furthermore, the processability of these nanocomposites can be facilitated by introducing CO_2. After processing, CO_2 is released and the polymer chains are reconfined onto the substrate, thus reinforcing polymer nanostructures for various end applications.

Acknowledgment. This work was partially supported by the NSF-sponsored Nanoscale Science and Engineering Center for Affordable Nanoengineering of Polymeric Biomedical Devices (NSEC-CANPBD) at The Ohio State University. We thank Jeffrey Ellis and Dr. David L. Tomasko for assistance on CO_2 absorption measurements of the polymer thin films.

References and Notes

(1) Wu, W.-l.; van Zanten, J. H.; Orts, W. J. *Macromolecules* **1995**, *28*, 771−4.
(2) Jones, R. A. L. *Nat. Mater.* **2003**, *2*, 645−646.
(3) Forrest, J. A.; Dalnoki-Veress, K. *Adv. Colloid Interface Sci.* **2001**, *94*, 167−195.
(4) Keddie, J. L.; Jones, R. A. L.; Cory, R. A. *Europhys. Lett.* **1994**, *27*, 59−64.
(5) Ellison, C. J.; Torkelson, J. M. *Nat. Mater.* **2003**, *2*, 695−700.
(6) Kawaguchi, D.; Tanaka, K.; Kajiyama, T.; Takahara, A.; Tasaki, S. *Macromolecules* **2003**, *36*, 1235−1240.
(7) van Zanten, J. H.; Wallace, W. E.; Wu, W.-l. *Phys. Rev. E* **1996**, *53*, R2053−R2056.
(8) Lin, E. K.; Kolb, R.; Satija, S. K.; Wu, W.-l. *Macromolecules* **1999**, *32*, 3753−3757.
(9) Tate, R. S.; Fryer, D. S.; Pasqualini, S.; Montague, M. F.; de Pablo, J. J.; Nealey, P. F. *J. Chem. Phys.* **2001**, *115*, 9982−9990.
(10) Torres, J. A.; Nealey, P. F.; de Pablo, J. J. *Phys. Rev. Lett.* **2000**, *85*, 3221−3224.
(11) Johnston, K. P.; Shah, P. S. *Science* **2004**, *303*, 482−483.
(12) Pham, J. Q.; Sirard, S. M.; Johnston, K. P.; Green, P. F. *Phys. Rev. Lett.* **2003**, *91*, 175503/1−17550.3/4.
(13) Gupta, R. R.; Lavery, K. A.; Francis, T. J.; Webster, J. R. P.; Smith, G. S.; Russell, T. P.; Watkins, J. J. *Macromolecules* **2003**, *36*, 346−352.
(14) Yang, Y.; Zeng, C.; Lee, L. J. *Adv. Mater.* **2004**, *16*, 560−564.
(15) Yang, Y.; Lee, L. J.; Lu, W. *J. Vac. Sci. Technol., B* **2005**, *23*, 3202−3204.
(16) Yang, Y.; Liu, D.; Xie, Y.; Lee, L. J.; Tomasko, D. L. *Adv. Mater.* **2007**, *19*, 251−254.
(17) Satomi, N.; Takahara, A.; Kajiyama, T. *Macromolecules* **1999**, *32*, 4474−4476.
(18) Kunz, K.; Stamm, M. *Macromolecules* **1996**, *29*, 2548−54.
(19) Karim, A.; Felcher, G. P.; Russell, T. P. *Macromolecules* **1994**, *27*, 6973−9.
(20) Rudoy, V. M.; Dement'eva, O. V.; Yaminskii, I. V.; Sukhov, V. M.; Kartseva, M. E.; Ogarev, V. A. *Colloid J.* (translation of *Kolloidn. Zh.)* **2002**, *64*, 746−754.
(21) Teichroeb, J. H.; Forrest, J. A. *Phys. Rev. Lett.* **2003**, *91*, 016104/1−01610.4/4.
(22) Russell, T. P. *Mater. Sci. Rep.* **1990**, *5*, 171−271.
(23) Lin, E. K.; Wu, W.-l.; Satija, S. K. *Macromolecules* **1997**, *30*, 7224−7231.
(24) Sharp, J. S.; Teichroeb, J. H.; Forrest, J. A. *Eur. Phys. J. E: Soft Matter* **2004**, *15*, 473−487.
(25) Hutcheson, S. A.; McKenna, G. B. *Phys. Rev. Lett.* **2005**, *94*, 076103/1−07610.3/4.
(26) Sirard, S. M.; Ziegler, K. J.; Sanchez, I. C.; Green, P. F.; Johnston, K. P. *Macromolecules* **2002**, *35*, 1928−1935.
(27) Koga, T.; Seo, Y. S.; Hu, X.; Shin, K.; Zhang, Y.; Rafailovich, M. H.; Sokolov, J. C.; Chu, B.; Satija, S. K. *Europhys. Lett.* **2002**, *60*, 559−565.
(28) Kuhlmann, T.; Kraus, J.; Muller-Buschbaum, P.; Schubert, D. W.; Stamm, M. *J. Non-Cryst. Solids* **1998**, *235−237*., 457−463.
(29) Zheng, X.; Sauer, B. B.; Van, Alsten, J. G.; Schwarz, S. A.; Rafailovich, M. H.; Sokolov, J.; Rubinstein, M. *Phys. Rev. Lett.* **1995**, *74*, 407−10.
(30) Jia, X.; McCarthy, T. J. *Langmuir* **2002**, *18*, 683−687.
(31) Zheng, X.; Rafailovich, M. H.; Sokolov, J.; Strzhemechny, Y.; Schwarz, S. A.; Sauer, B. B.; Rubinstein, M. *Phys. Rev. Lett.* **1997**, *79*, 241−244.
(32) Yang, Y.; Xie, Y.; Kang, X.; Lee, L. J.; Kniss, D. A. *J. Am. Chem. Soc.* **2006**, *128*, 14040−14041.

MA061492O